COMBUSTION RESEARCH ACTIVITIES AT THE GAS TURBINE RESEARCH INSTITUTE

Shao Zhongpu
Gas Turbine Research Institute
Jiangyou County of Sichuan, People's Republic of China

The Gas Turbine Research Institute (GTRI) is responsible mainly for basic research in aeronautical propulsion. The combustion research activities primarily cover the following areas: annular diffuser for the turbofan augmentor, combustor ignition performance, combustor airflow distribution, fuel injectors, vaporizer fuel injector, and airblast atomizer.

RESEARCH ON THE ANNULAR DIFFUSER FOR THE TURBOFAN AUGMENTOR

It is well known that the inlet velocity profile has a very strong influence on diffuser performance. The inlet velocity and temperature profiles are not uniform: both change with flight condition. The diffuser enlarges the inlet velocity distortion; that is, the nonuniformity of the velocity increases with the diffusion process occurring in the diffuser. The nonuniform inlet velocity profile encourages the airstream to separate from the diffuser wall or inner cone, induces flame stabilization in the separated flow region, and causes augmentor components to burn or to induce combustion instability. To obtain a desirable fuel-air distribution, it is necessary to understand the velocity and temperature profiles in the augmentor. In other words, since the velocity and temperature profiles at the exit of the diffuser must be known some experimental research was carried out on the annular diffuser of the turbofan augmentor.

The test model and the instrumentation locations are shown in figure 1. The test was run at the following conditions:

(1) Inlet Mach number, 0.08 to 0.60
(2) Inlet temperature, 300 to 600 K
(3) Inlet Reynolds number, $>5\times10^4$
(4) Diffuser outlet to inlet area ratio, 1.54
(5) Inner to outer annular area ratio, ≈1.0
(6) Inner cone, three configurations
(7) Cone angles, 20°, 30°, and 40°

The static-pressure recovery coefficients, velocity profiles, and temperature profiles along the axial distance were measured. The flow separation in the diffuser was studied by tuft observation method for low-temperature airflow under different inlet outer-inner velocity ratios and different inner-cone configurations. Typical inlet velocity and temperature profiles of the diffuser are shown in figures 2 and 3.

We found the following results:

(1) Within the range of the test Mach number (M_i or $M_e < 0.6$), the static-pressure recovery coefficients at different axial stations were independent of Mach number. As shown in figure 4, the inlet Mach number had little influence on the diffuser internal flow. Thus, the effect of inlet Mach number

C-2

can be neglected when testing or analyzing the performance of an annular diffuser for a turbofan augmentor.

(2) We also obtained an important nondimensional flow parameter,

$$S_D = \left(\bar{\rho}_e \bar{v}_e^2\right)\left(\bar{\rho}_i \bar{v}_i^2\right) = \left(\bar{v}_e \bar{T}_e^{-0.5}\right)\left(\bar{v}_i \bar{T}_i^{-0.5}\right)$$

If we use a diffuser with the same geometry and a similar inner velocity profile and maintain S_D = constant, then the change of static-pressure recovery coefficients and nondimensional, combined velocity-temperature combination distributions along the diffuser axial distance is the same, regardless of whether the test is done with low- or high-temperature air, as shown in figures 5 and 6. It is possible to use the low-temperature test to simulate real turbofan augmentor diffuser flow; low-temperature airflow separation can also be used to understand high-temperature airflow separation.

RESEARCH ON COMBUSTOR IGNITION PERFORMANCE

Under the high-altitude relight condition, the combustion chamber inlet pressure can be as low as 0.2 kg/cm^2, and the inlet temperature can be as low as -50 °C. Because it is important for combustion engineers to understand the relation between ignition performance and combustor inlet parameters, we studied the effect of inlet parameters on the ignition performance of combustors with different fuel-injection systems.

This test was performed on the high-altitude ignition test rig shown in figure 7. Three combustor configurations were used. The first configuration was a gas turbine combustor with a pressure swirl atomizer. (This combustor is similar to a JT-3D engine combustor with one flame tube.) The second configuration was a one-quarter sector of a full annular combustor with three T-shaped vaporizers, as shown in figure 8. The third configuration was similar to the second one - the only difference being that the three vaporizers had been replaced by three airblast atomizers.

A high-energy ignition plug was used for every configuration. The stored energy of the ignition system was 20 J, 12 J, and 8 J, respectively. The ignition procedures were repeated three times under every test condition. If all three ignitions were successful, then each was judged a successful ignition at its specific condition.

We drew the following conclusions from this experiment:

(1) The inlet pressure has a significant effect on the ignition performance of the combustors. Figure 9 shows the optimum fuel-air ratio as a function of inlet pressure for the three configurations. From figure 9 we can see the effect of the inlet air pressure on ignition performance of the combustors, especially at low pressure.

(2) The inlet air temperature has a strong effect on the ignition performance of the combustors. The effects of the inlet air temperature on maximum ignitable reference velocity and on optimum fuel-air ratio for the three configurations are shown in figures 10 and 11. As the inlet air temperature decreases, the maximum ignitable reference velocity decreases. At higher inlet

air temperatures, the effect of the inlet air temperature on the optimum ignitable fuel-air ratio is very weak; however, at lower inlet air temperatures the effect is very strong, especially for the vaporizer combustor.

Figures 12(a), (b), and (c) show the combined effects of inlet air pressure and temperature on ignition performance for the three configurations.

EXPERIMENTAL STUDY ON AIRFLOW DISTRIBUTION OF THE COMBUSTOR

The airflow distribution characteristics of a combustor directly affect the performance of the combustor such as combustion efficiency, range of stable operation, and temperature profile at the combustor exit. A 90° segment of the annular combustor was used for this study. The test assembly is shown in figure 13.

The goals of the study were as follows:

(1) To determine the effect of Mach number at the combustor inlet on the airflow distribution at an air temperature of 291 K
(2) To compare the changes of airflow distributions with and without burning in the combustor

Figure 13 shows the eight instrumentation sections on the test assembly. The flow rate G_{hi} through the holes on the wall of the flame tube can be calculated as follows:

$$G_{hi} = C_{di} A_{hi} \sqrt{2g\gamma \Delta P}$$

where

C_{di} airflow discharge coefficient of the holes

A_{hi} area of the holes

γ specific gravity of air

ΔP pressure drop through the holes, $= P^{*}_{ai} - P_{li}$

g acceleration of gravity

The flow rate (in percent) through each row of holes that is relative to the total is

$$\bar{G}_i = 100\left(G_{hi} \Big/ \sum_{i=1}^{N} G_{hi}\right)$$

The relative area (in percent) of the holes of each row of holes is

$$\bar{A}_i = 100\left(A_{hi} \Big/ \sum_{1}^{N} A_{hi}\right)$$

The following conclusions were obtained from this experimental study:

(1) At the range tested, there is no apparent influence on the airflow distribution by the Mach number at the combustor inlet, as shown in figures 14(a) and (b).

(2) Under the conditions

$$T^*_{in} = 291 \text{ K}$$

$$T^*_{ex}/T^*_{in} = 1 \sim 2.44$$

the airflow distributions have no obvious change, regardless of whether burning is present or not, as shown in figures 15(a) and (b). However, we are not certain that this would be true under real operating conditions.

EXPERIMENTAL STUDY ON FUEL INJECTORS

The fuel injector is one of the most important components of a combustor or afterburner. In order to determine the effects of geometric parameters, airflow parameters, and fuel rate on the fuel-spray characteristics, we have made an initial study of a vaporizer and an airblast atomizer.

The test rig assembly is shown in figure 16. The airflow rate G_a through the fuel injector was measured by a turbine flowmeter. The air velocity at the injector exit was

$$V_a = G_a(R)T_2/AP$$

The fuel rate G_f was also obtained by a turbine flowmeter where the air-fuel ratio is given by

$$AFR = G_a/G_f$$

The Sauter mean diameter (SMD) of the fuel spray drops was measured by a Malvern laser particle sizer.

EXPERIMENTAL STUDY ON VAPORIZER FUEL INJECTOR

Since we tried to understand the spray characteristics - not the vaporizing condition - for different vaporizer fuel injectors, we studied the spray characteristics under low inlet air temperature only and did not heat the vaporizer. Some of the test vaporizers are shown in figures 17 and 18.

The following conclusions were made:

(1) The air velocity V_a at the vaporizer exit is the most important factor affecting fuel atomization. As shown in figure 19, SMD decreases with increasing V_a.

(2) The effect of air-fuel ratio on fuel atomization is related to the air velocity at the vaporizer exit. If AFR <4 and the air velocity is low, then, as AFR increases, SMD will decrease. When the air velocity is much higher, the effect is not apparent, as shown in figures 20 and 21.

(3) The method and the pressure of injecting fuel into the vaporizer has no significant influence on fuel atomization, as shown in figure 22.

EXPERIMENTAL STUDY OF THE AIR-BLAST ATOMIZER

The geometric parameters of the airblast atomizers we have tested are listed in the following table:

Number	Inner channel feature	Outer channel feature	Total exit area, mm
0	Straight flow	Tangent flow holes	295.4
11	With swirl vane	Tangent flow holes	295.4
21	Straight flow	Rectangular flow holes	359.5
7	Straight flow	Rectangular flow holes	295.4
17	Straight flow	Rectangular flow holes	235.1
10	With swirl vane	Rectangular flow holes	295.4

The test atomizers are shown in figures 23 and 24.

The conclusions were as follows:

(1) Under the test conditions, SMD decreased with increasing airspray velocity, as shown in figure 25.

(2) When AFR <4, SMD decreased with increasing AFR. When AFR >4, there was no significant influence on SMD, as shown in figure 26.

(3) For the same conditions, SMD decreased as the exit area of the atomizer increased (fig. 27). The reason for such a result has not been determined yet.

There are many interesting subjects related to combustion such as combustor exit temperature profile, the procedure to control exhaust emission, combustor diagnostics, swirl combustion, and cooling techniques. We are prepared to do further experimental study.

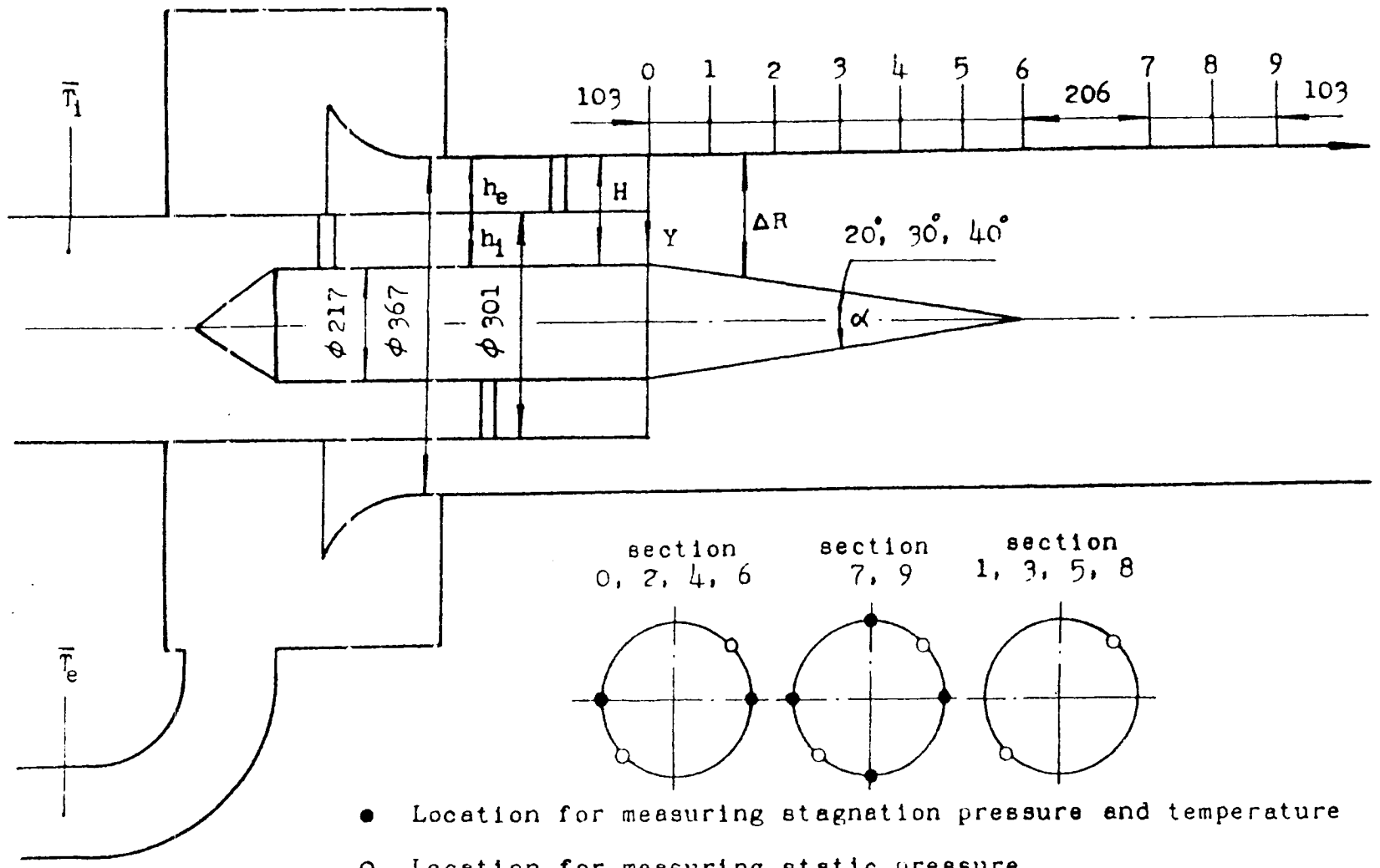

Figure 1. - Test section and measurement locations.

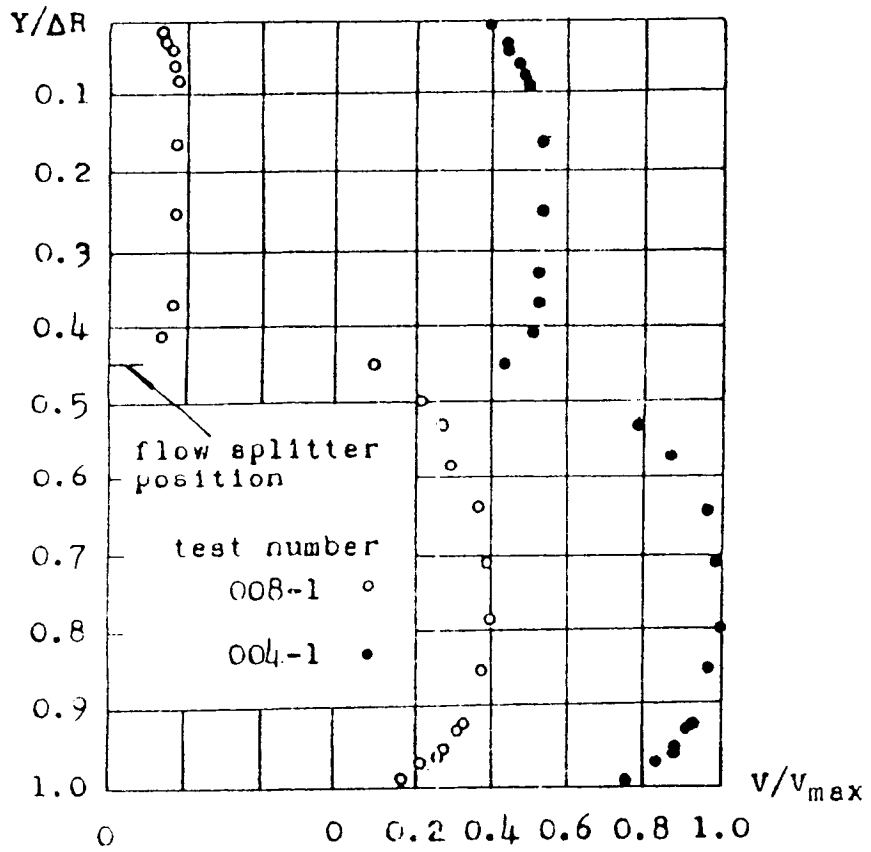

Figure 2. - Typical, nondimensional diffuser inlet velocity profile.

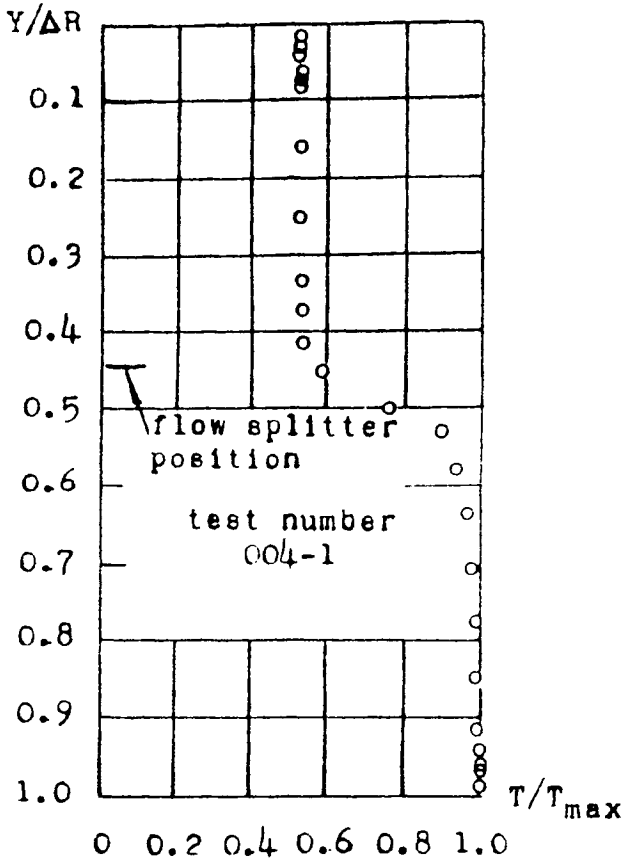

Figure 3. - Typical, nondimensional diffuser inlet velocity profile.

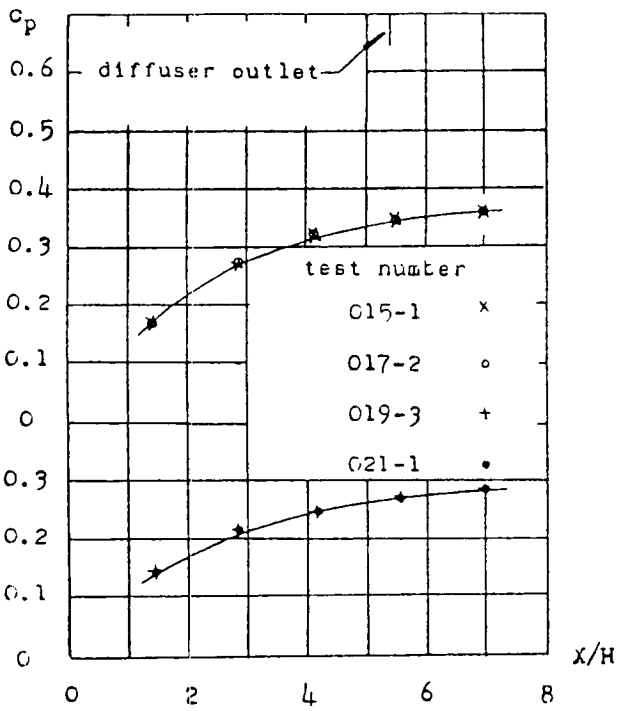

Figure 4. - Static-pressure recovery coefficient as function of nondimensional axial distance;
$\bar{T}_i \sqrt{T_e}$ = constant, $\bar{V}_i \sqrt{V_e}$ = constant.

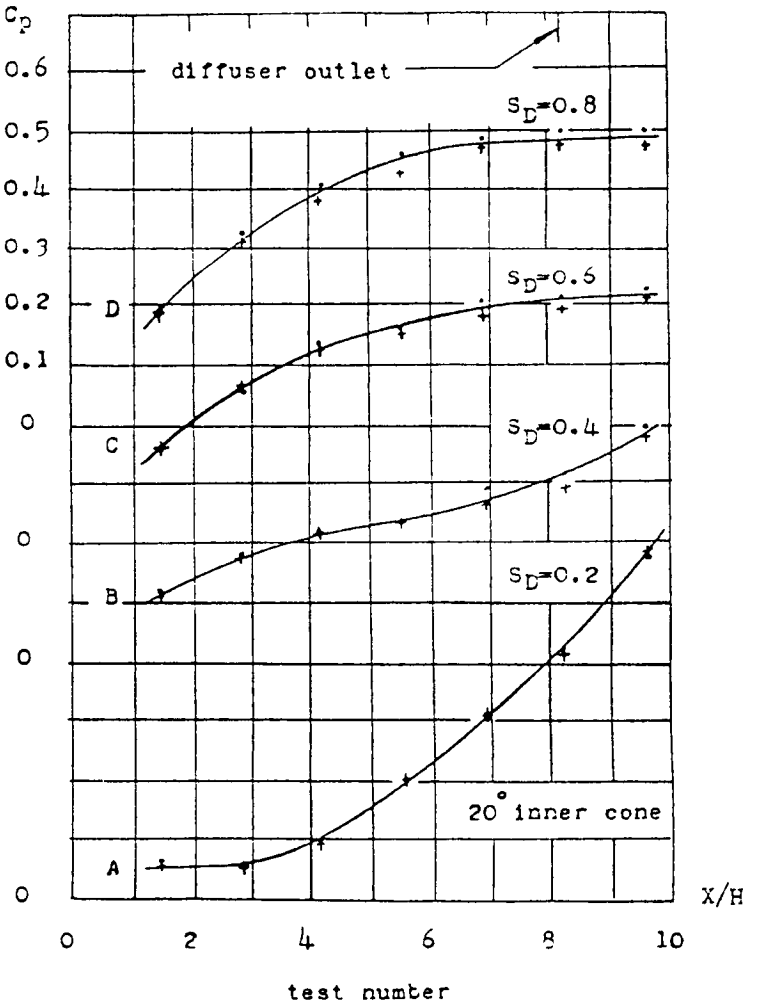

Figure 5. - Static-pressure recovery coefficient as function of diffuser axial distance under different nondimensional diffuser flow parameters. A, 024-1 + 024-2; B, 024-3 + 024-4; C, 024-5 + 024-6; D, 024-7 + 024-8.

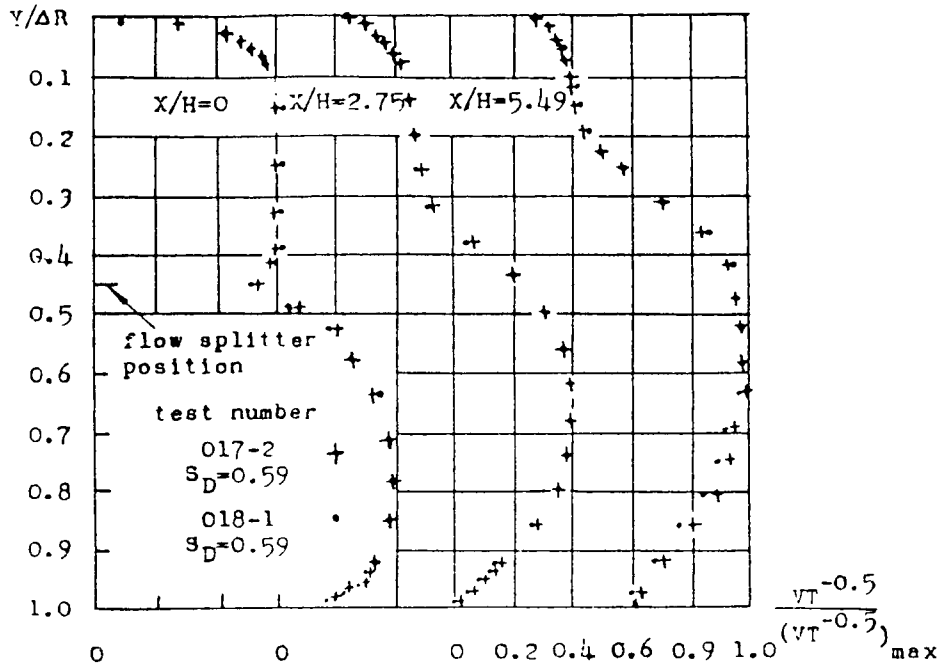

Figure 6. - Nondimensional velocity-temperature combination distribution under constant S_D value for low-temperature and high-temperature tests.

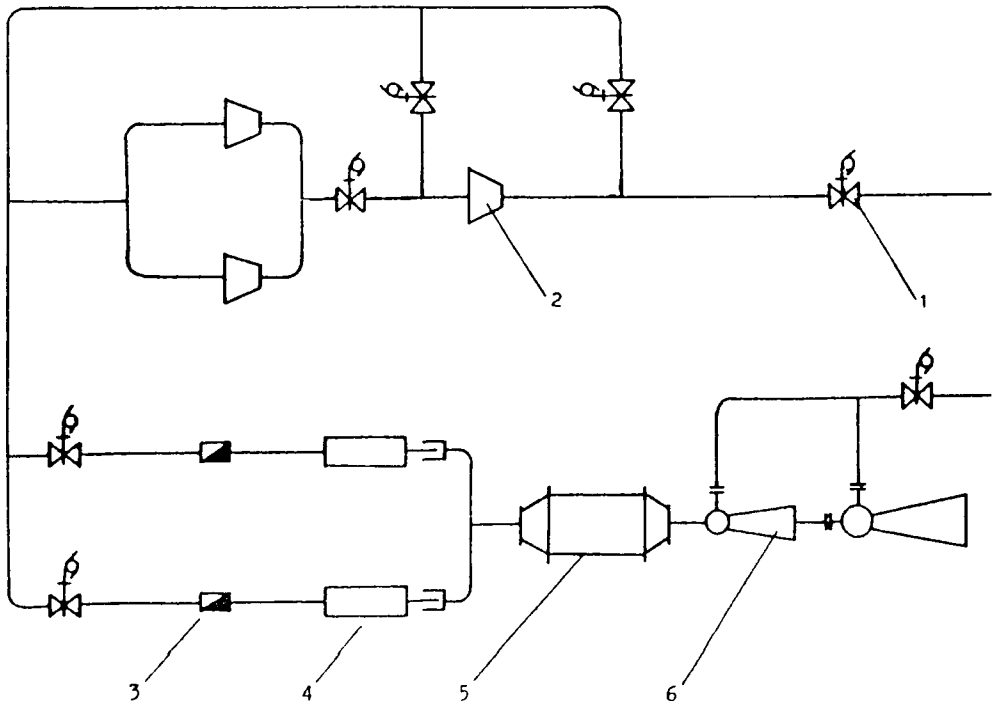

Figure 7. - Air system for high-altitude ignition rig. Solenoid valve, 1; expansion turbine, 2; flow measurement nozzle, 3; test combustor, 4; cooling device, 5; ejector, 6.

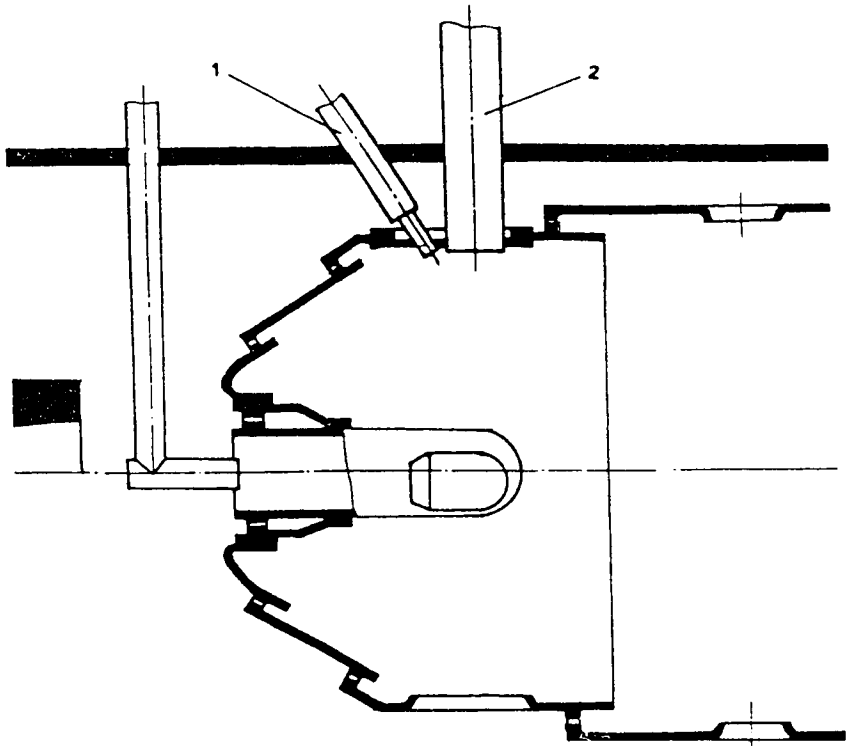

Figure 8. - Installation of ignition plug in vaporizer combustor. Starting fuel injector, 1; high-energy ignition plug, 2.

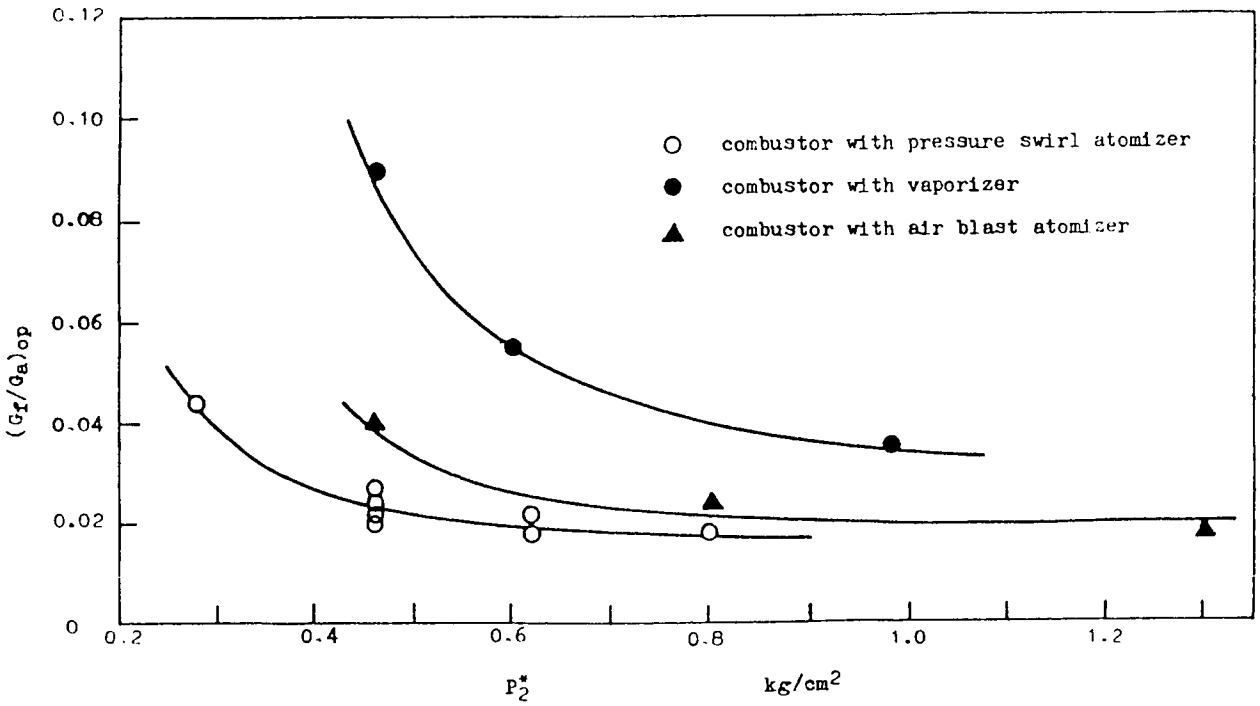

Figure 9. - Optimum fuel-air ratio versus inlet pressure; $T_2^* = 293$ K.

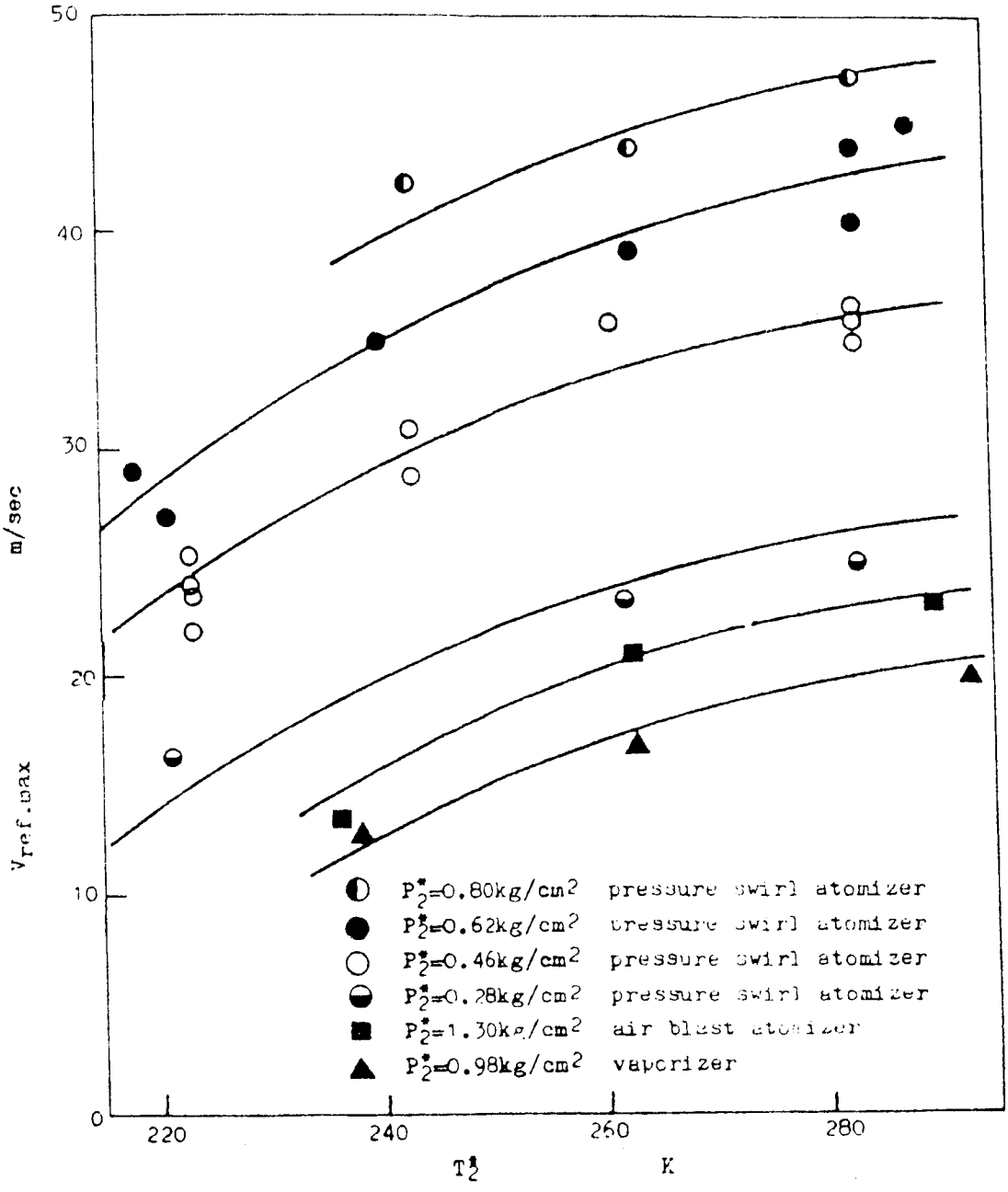

Figure 10. - Effect of inlet temperature on maximum ignitable reference velocity.

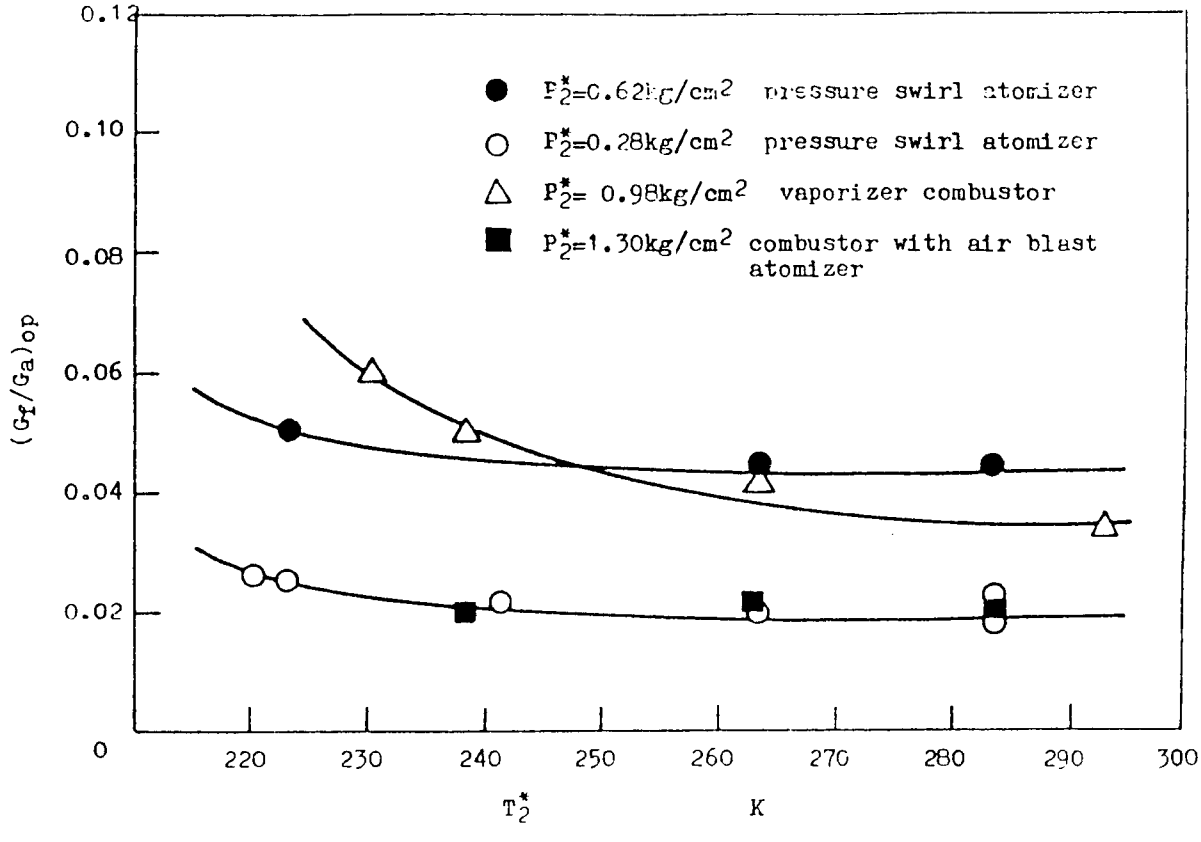

Figure 11. - Effect of inlet temperature on optimum fuel-air ratio.

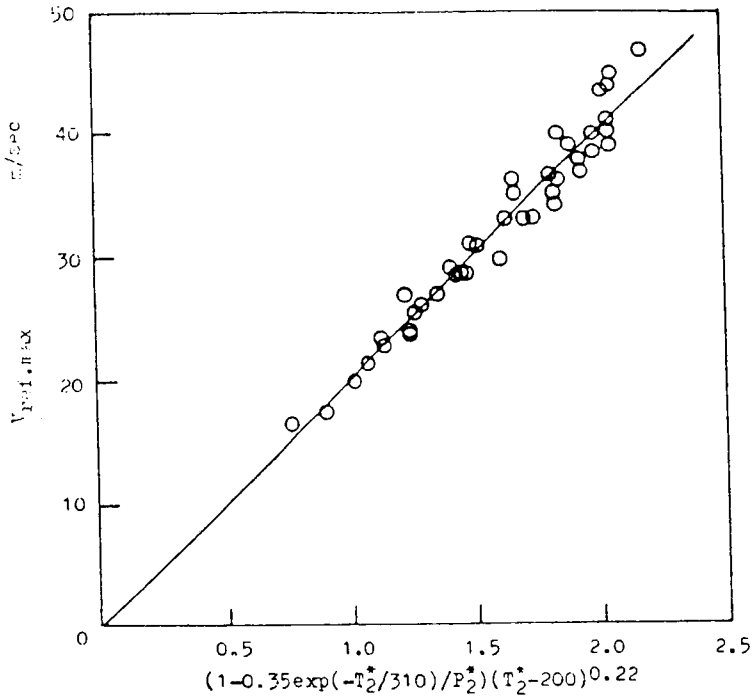

(a) Experimental combustor with pressure swirl atomizer.

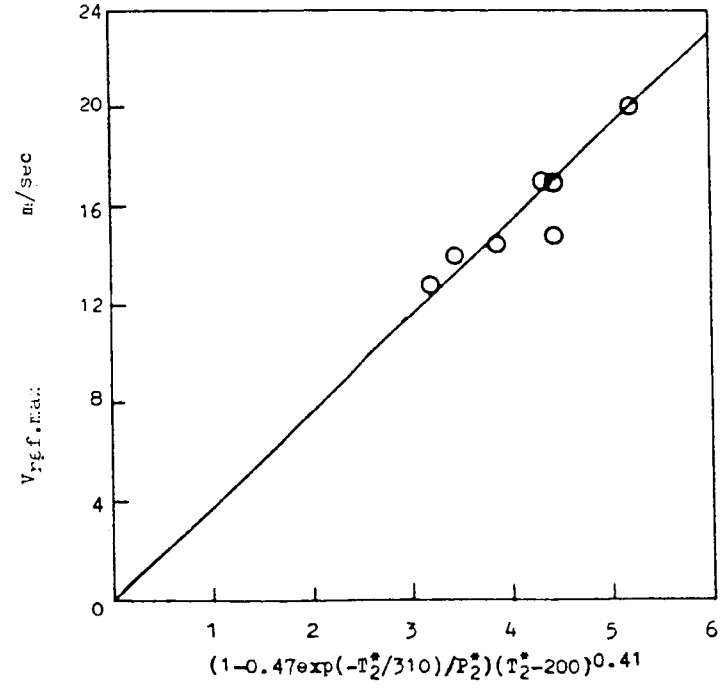

(b) Experimental combustor with vaporizer.

Figure 12. - Correlation of maximum ignitable reference velocity with inlet parameters.

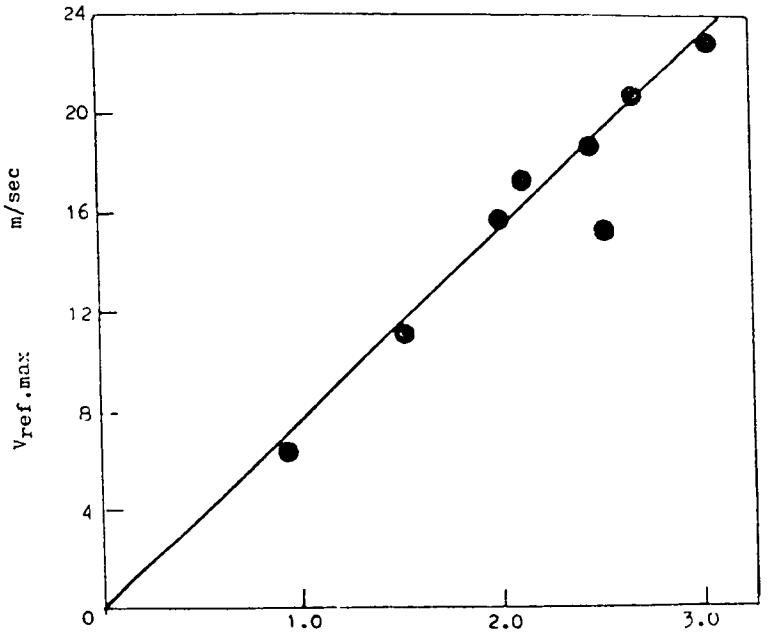

(c) Experimental combustor with air-blast atomizer.

Figure 12. - Concluded.

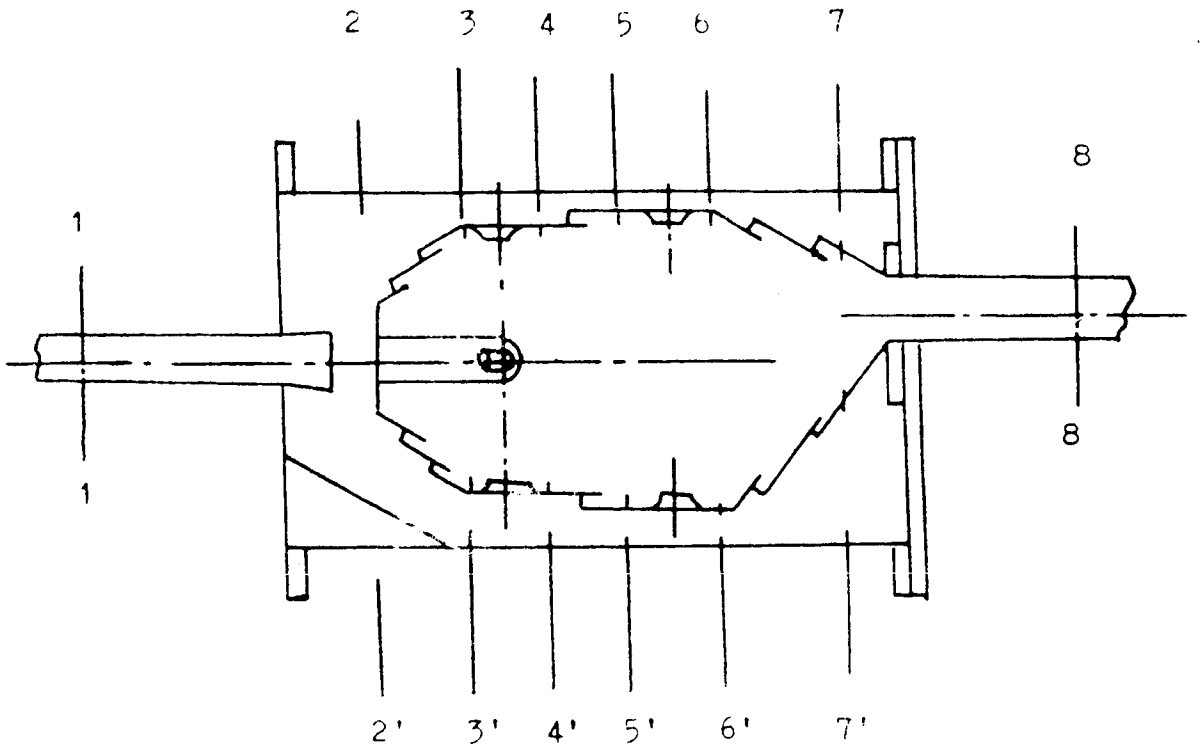

Figure 13. - Test combustor and instrumentation on locations.

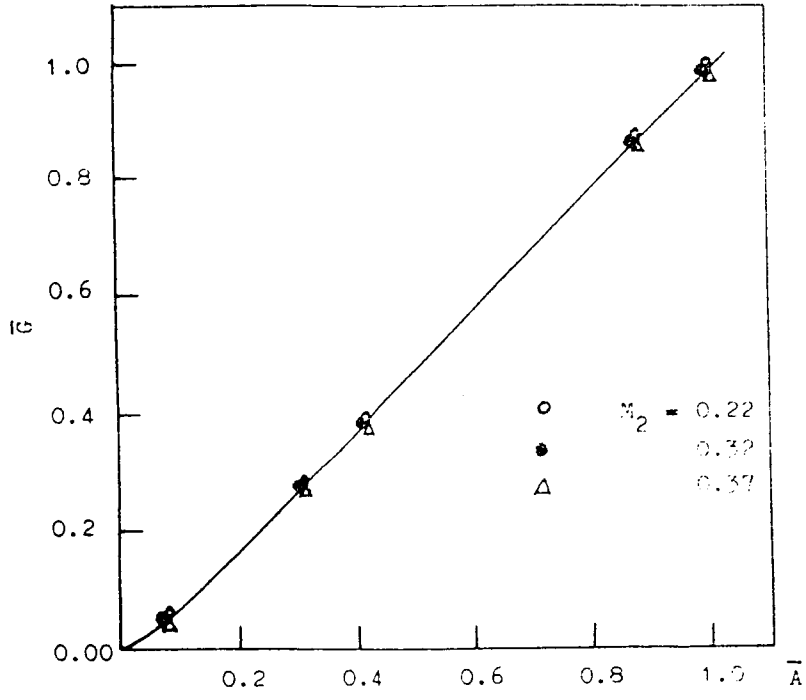

(a) Outer annulus.

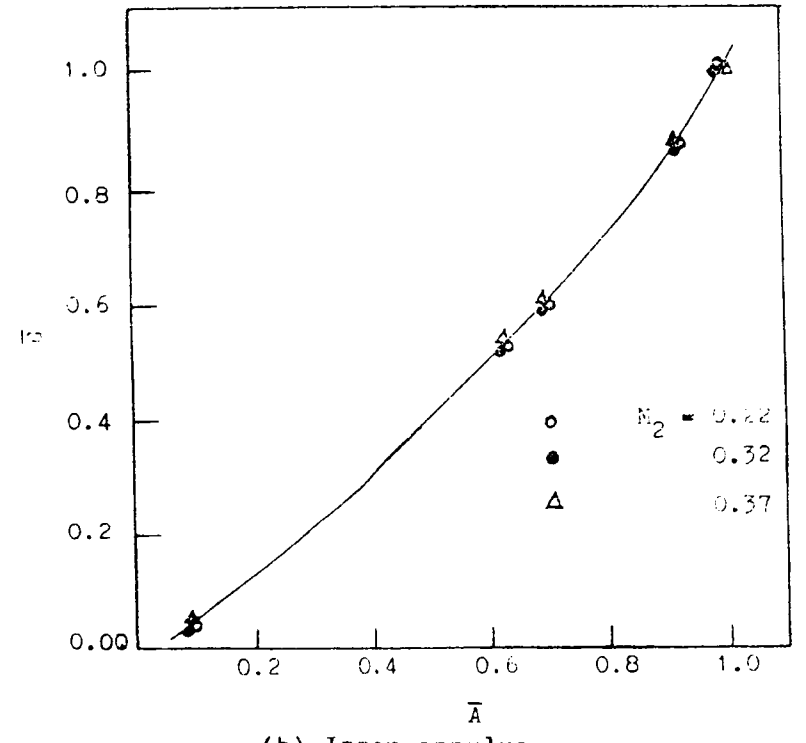

(b) Inner annulus.

Figure 14. - Effect of Mach number on air-flow distribution of annulus; T^*_{in} = 291 K, T^*_{ex}/T^*_{in} = 1.

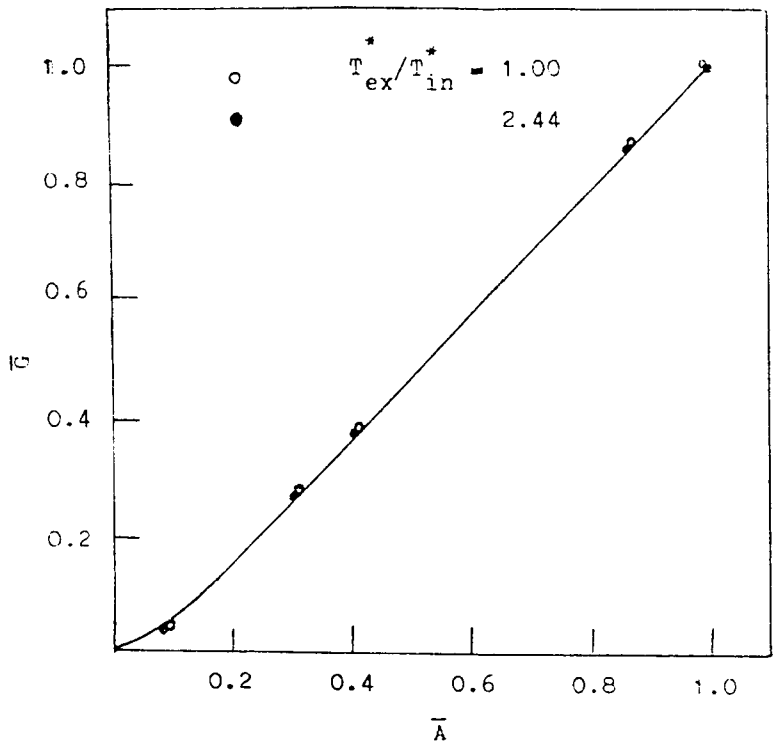

(a) Outer annulus.

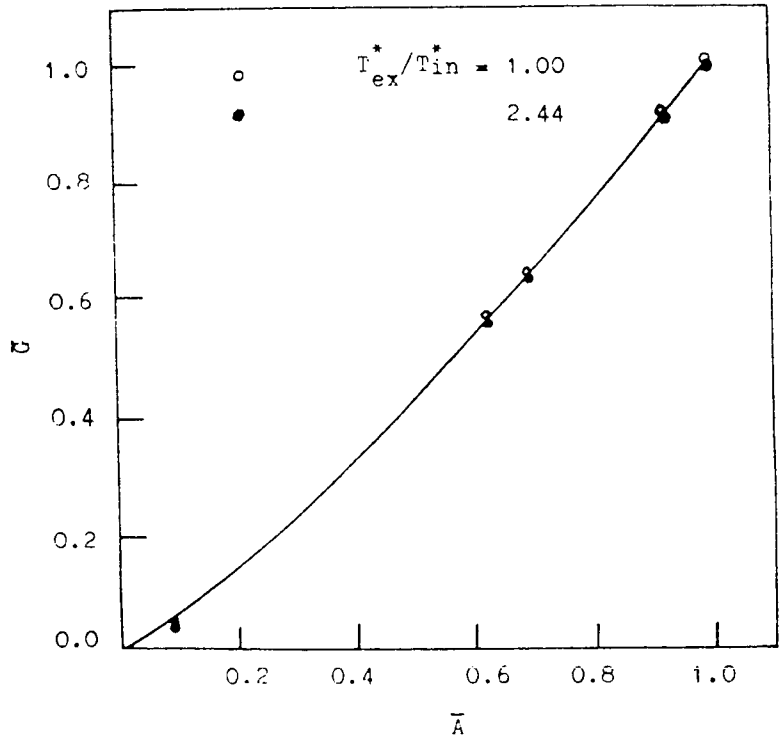

(b) Inner annulus.

Figure 15. - Effect of combustion on air-flow distribution of annulus.

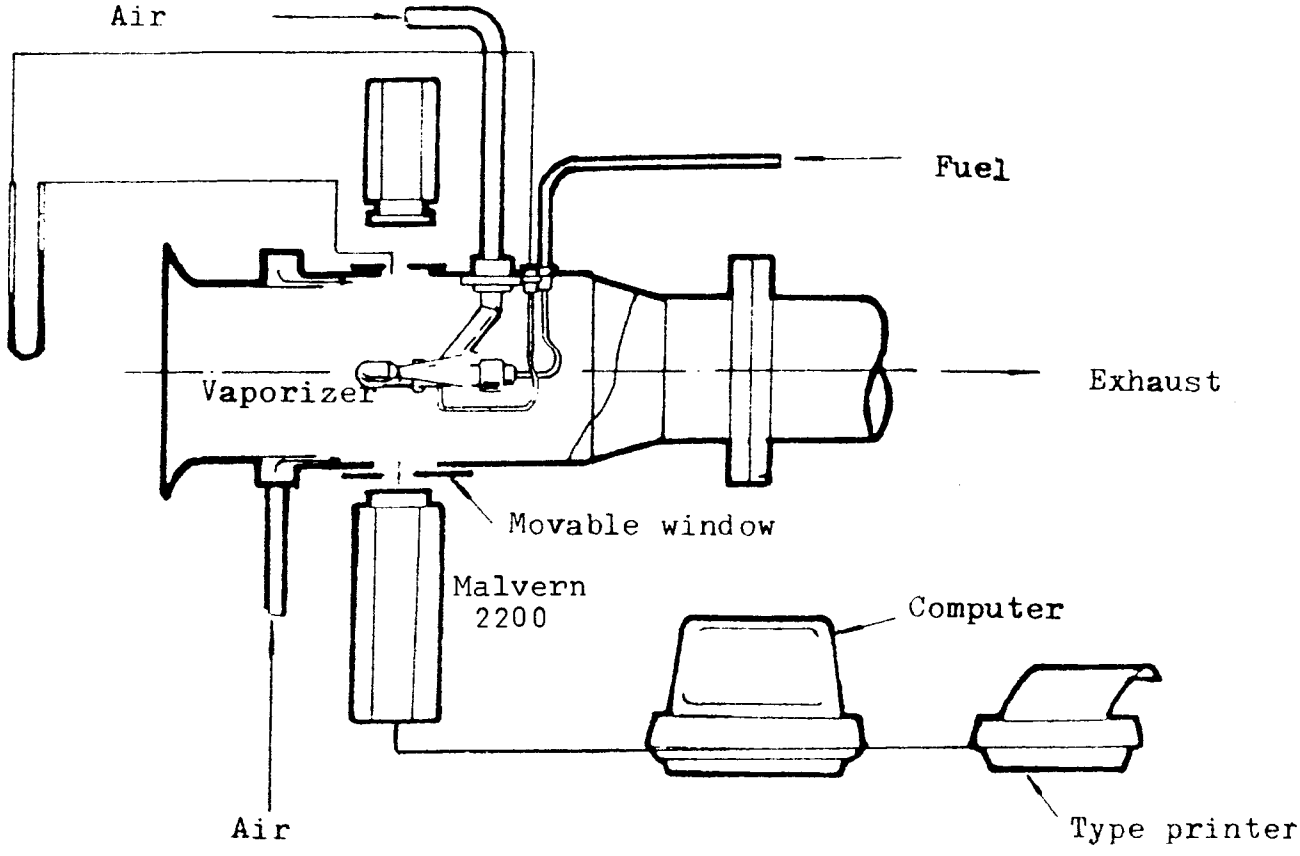

Figure 16. - Test rig assembly.

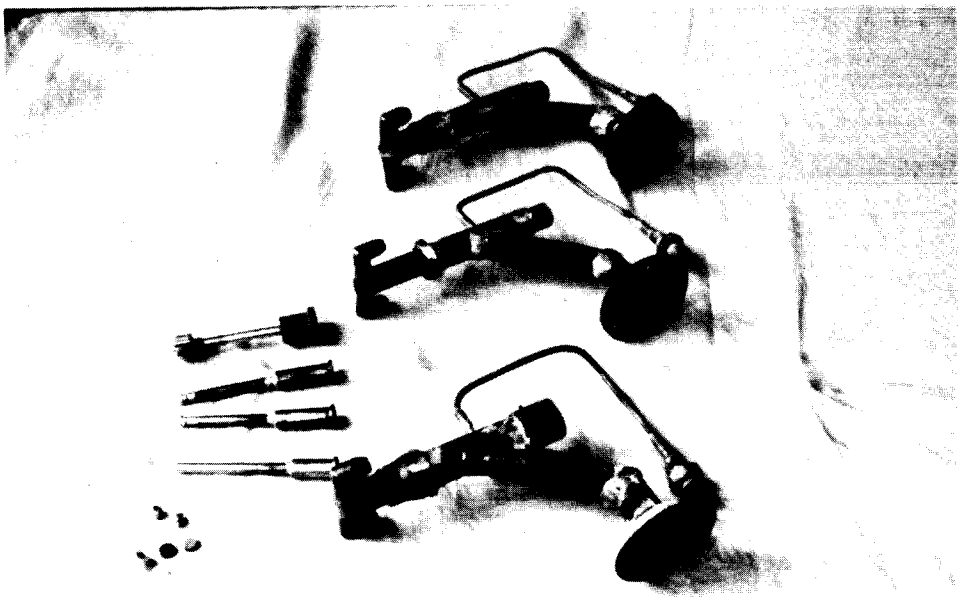

Figure 17. - Test vaporizers.

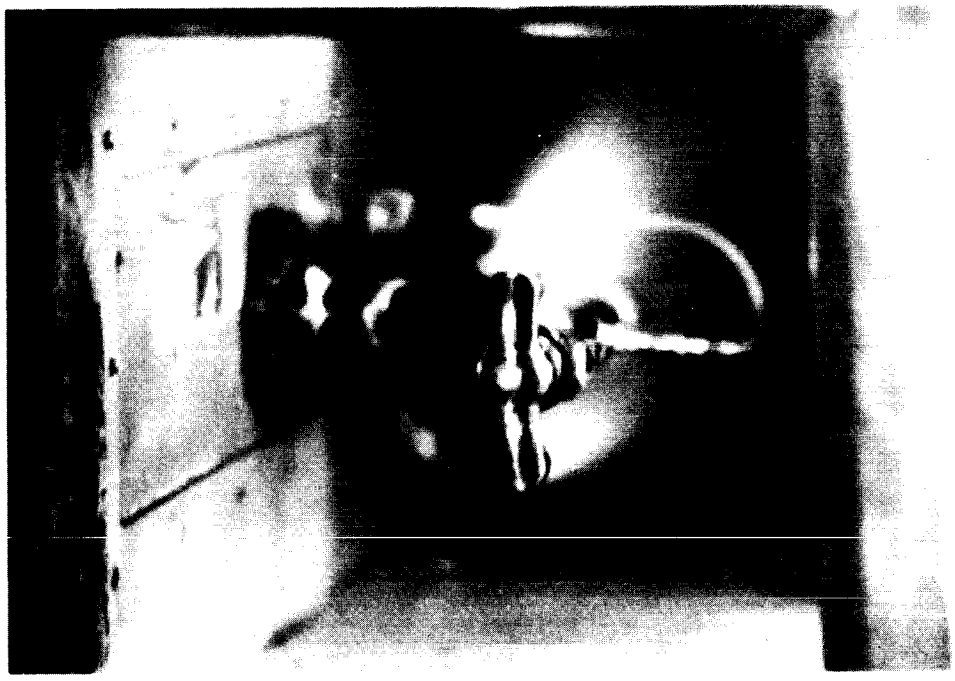

Figure 18. - Test vaporizer.

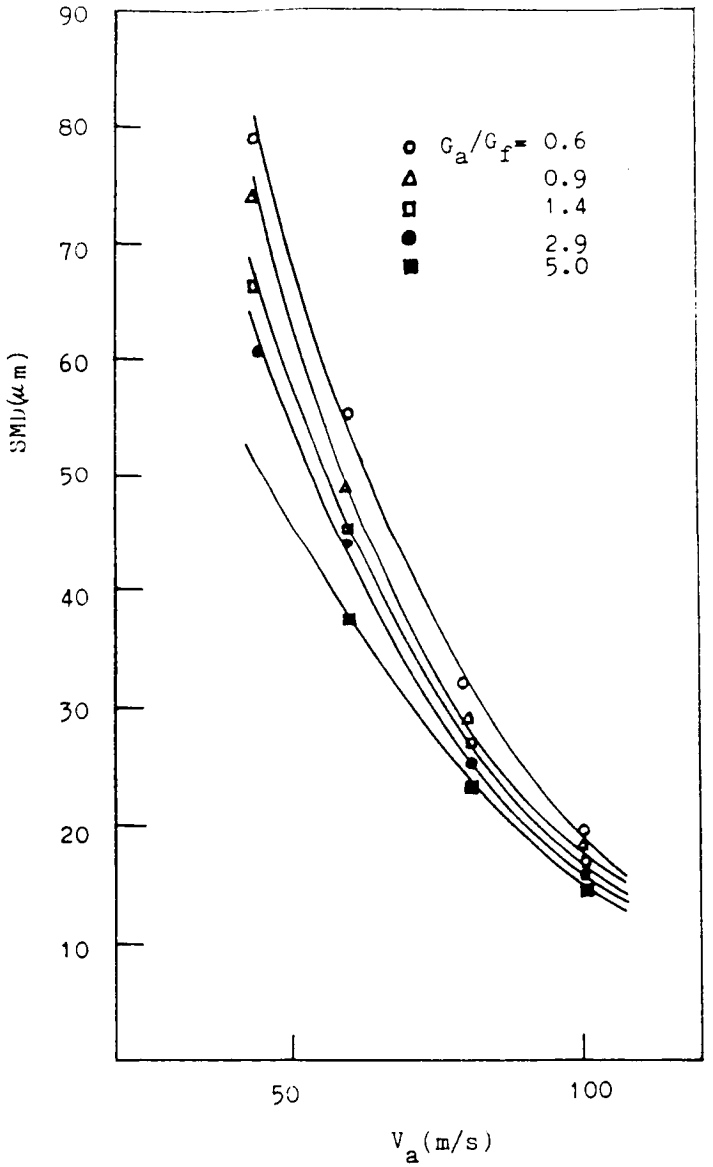

Figure 19. - Effect of air velocity on SMD for vaporizer fuel injector #1.

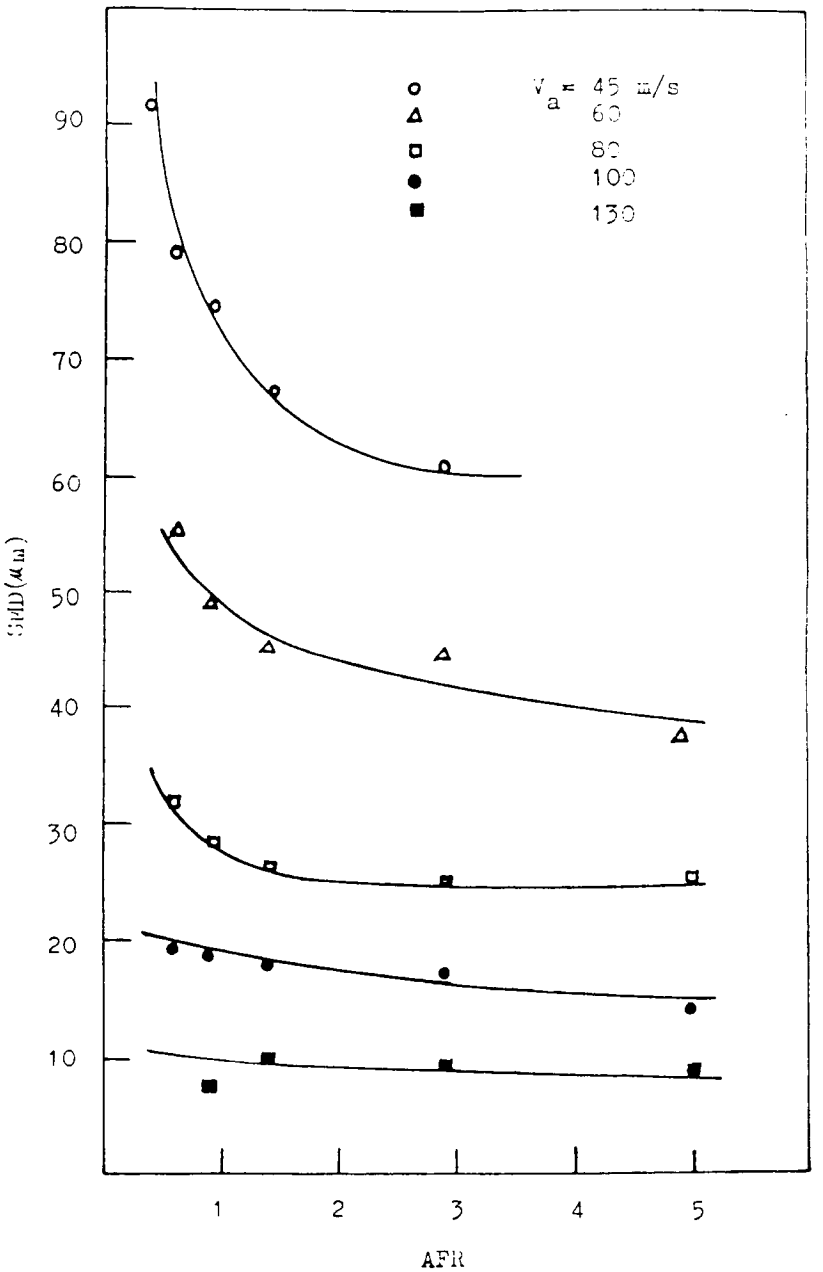

Figure 20. - Effect of air-fuel ratio on SMD for vaporizer fuel injector #1; L = 50 mm.

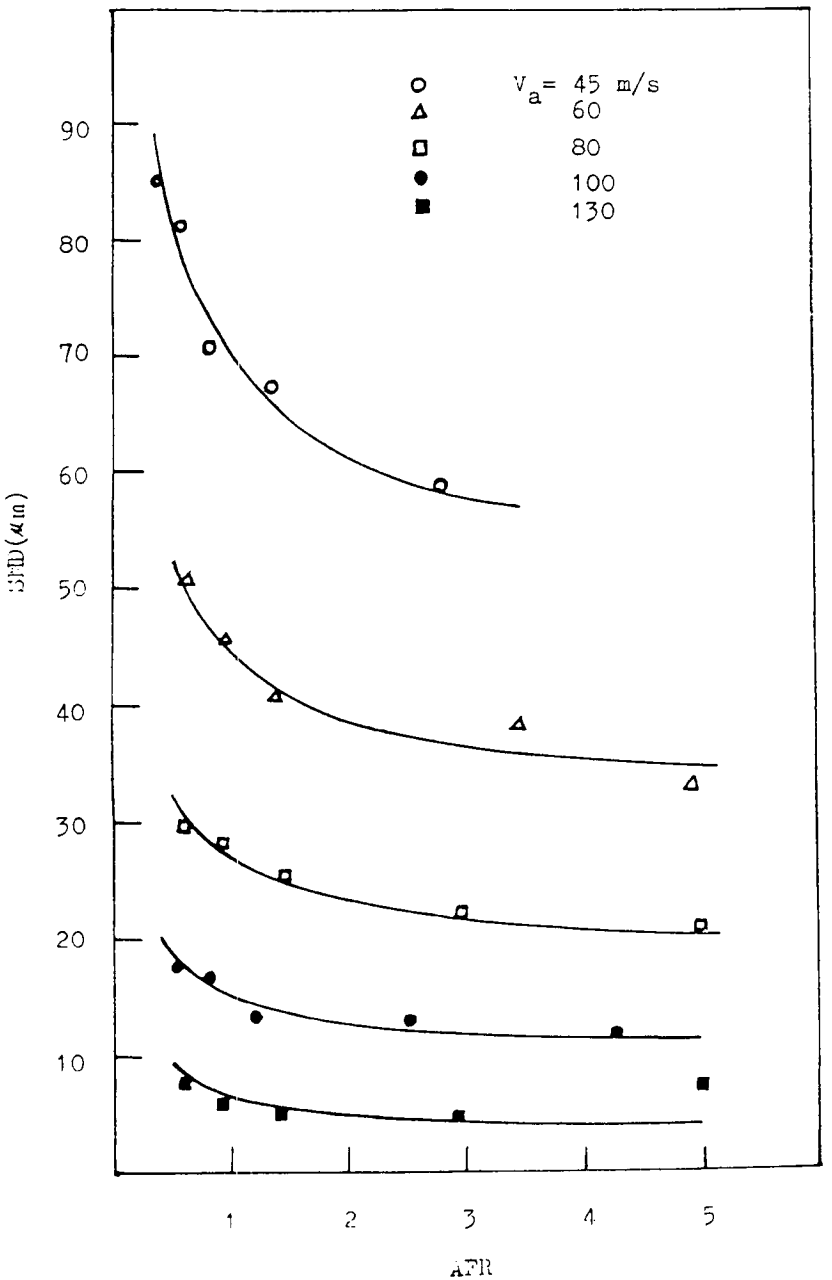

Figure 21. - Effect of air-fuel ratio on SMD for vaporizer fuel injector #12; L = 50 mm.

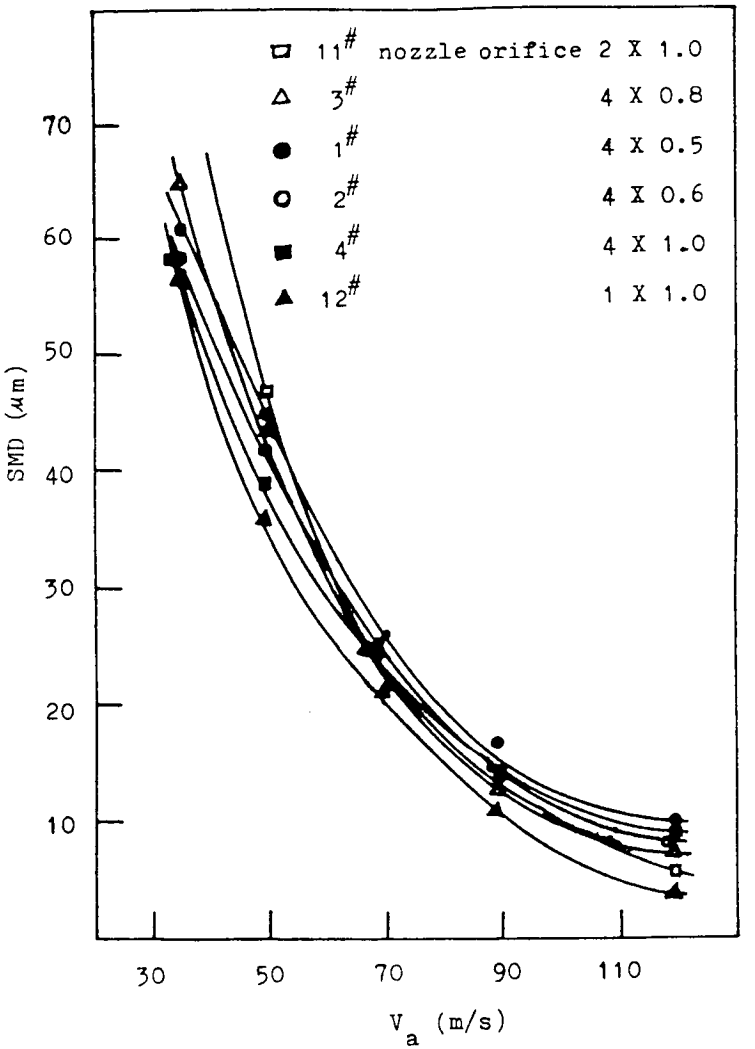

Figure 22. - Effect of spray method on SMD. Vaporizer D x d = 18 x 7; L = 50 mm; AFR = 2.9.

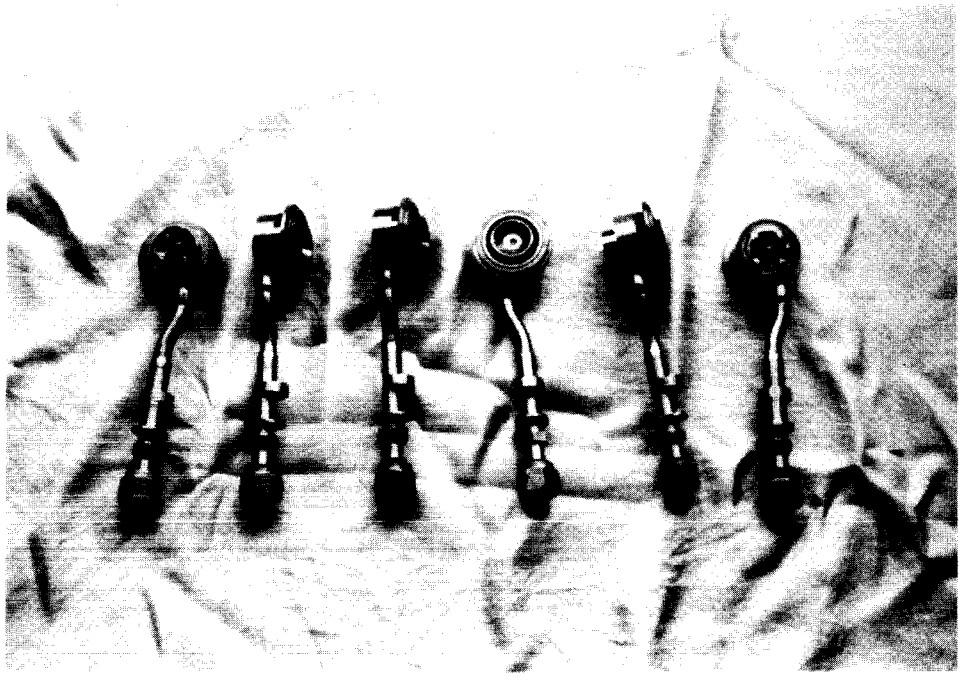

Figure 23. - Test air-blast atomizer.

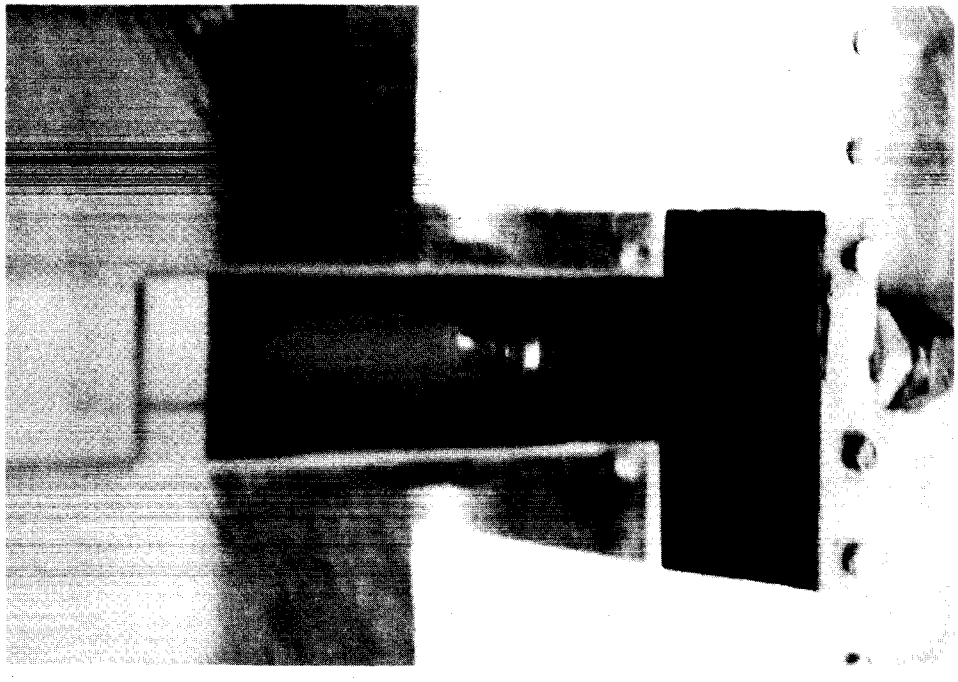

Figure 24. - Test atomizer.

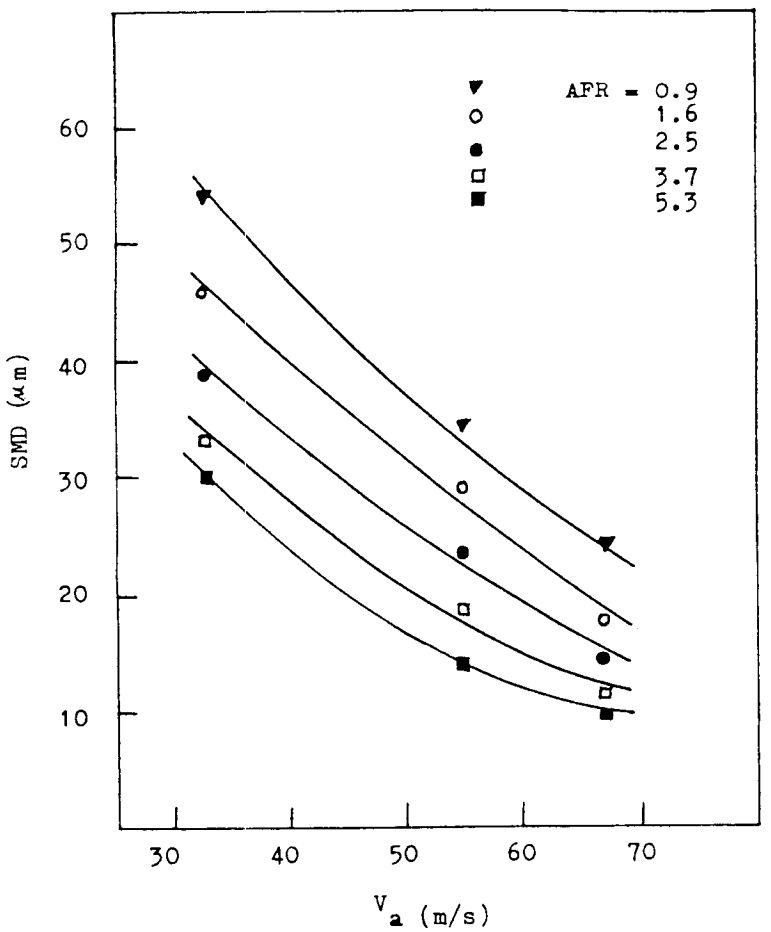

Figure 25. - Effect of air velocity on SMD for air-blast atomizer #11; L = 38 mm.

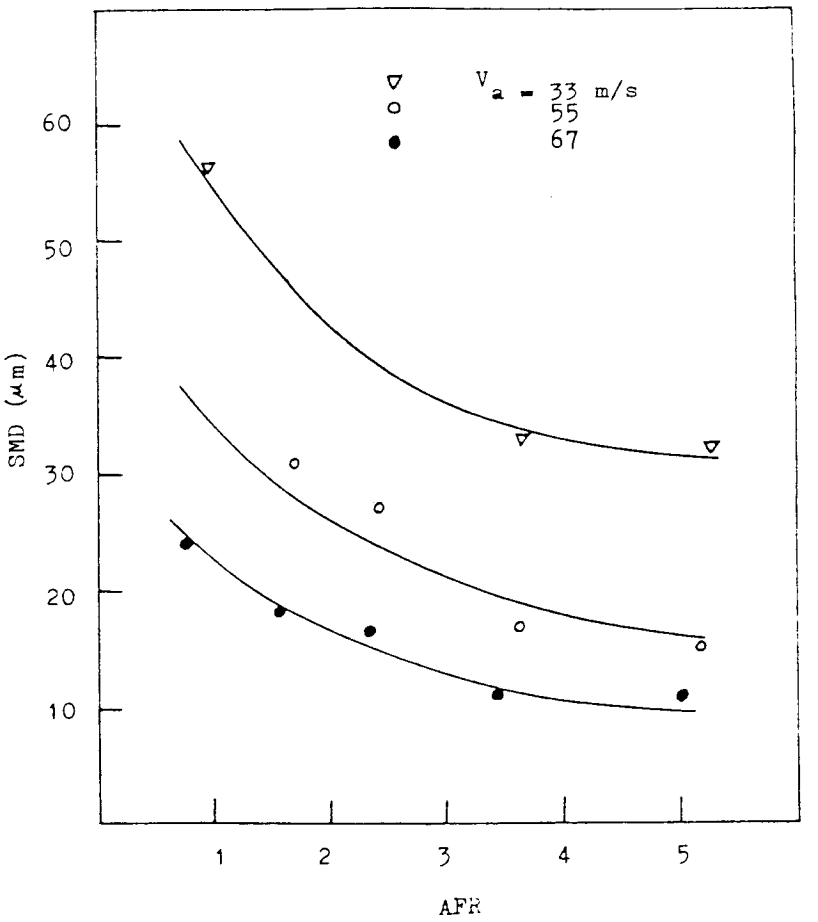

Figure 26. - Effect of air-fuel ratio on SMD for air-blast atomizer #11; L = 38 mm.

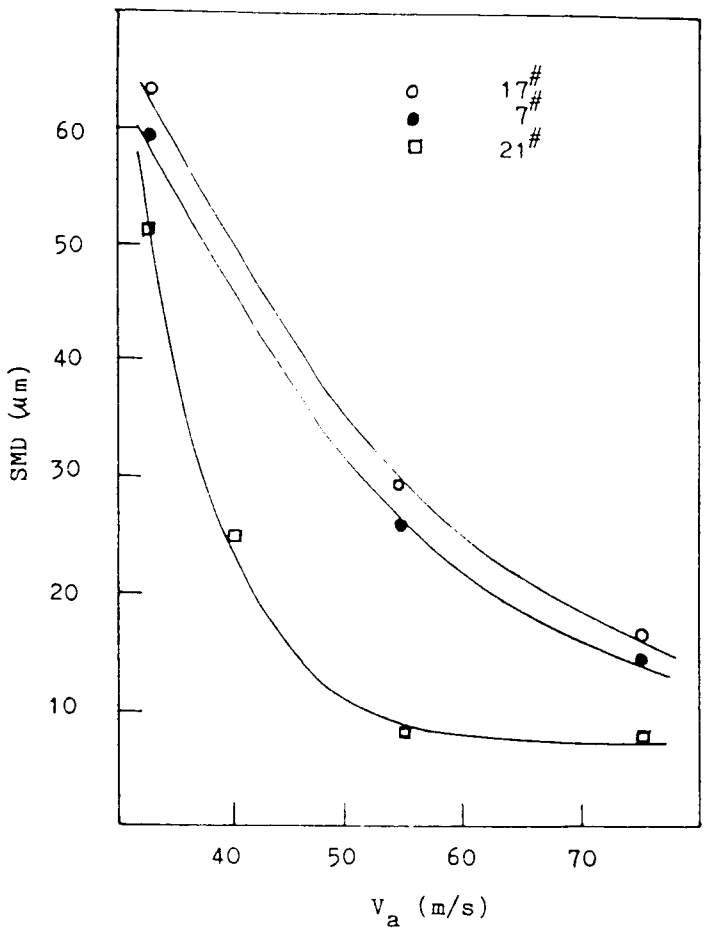

Figure 27. - Effect of nozzle outlet area on SMD; AFR = 2.5.